Mechanism and Activity of Ruthenium Olefin Metathesis Catalysts

Melanie S. Sanford, Jennifer A. Love, and Robert H. Grubbs*

Contribution from the Arnold and Mabel Beckman Laboratories for Chemical Synthesis, Division of Chemistry and Chemical Engineering, California Institute of Technology, Pasadena, California 91125

Received March 8, 2001

Abstract: This report details the effects of ligand variation on the mechanism and activity of ruthenium-based olefin metathesis catalysts. A series of ruthenium complexes of the general formula $L(PR_3)(X)_2Ru{=}CHR^1$ have been prepared, and the influence of the substituents L, X, R, and R^1 on the rates of phosphine dissociation and initiation as well as overall activity for olefin metathesis reactions was examined. In all cases, initiation proceeds by dissociative substitution of a phosphine ligand (PR_3) with an olefinic substrate. All of the ligands L, X, R, and R^1 have a significant impact on initiation rates and on catalyst activity. The origins of the observed substituent effects as well as the implications of these studies for the design and implementation of new olefin metathesis catalysts and substrates are discussed in detail.

Introduction

Over the past decade, olefin metathesis has emerged as a powerful method for the formation of carbon−carbon double bonds.[1] In particular, the ruthenium-based catalyst $(PCy_3)_2(Cl)_2Ru{=}CHPh$ (**1**) (Figure 1)[2] has been used extensively in organic and polymer chemistry due to its high reactivity with olefinic substrates in the presence of most common functional groups.[3] The mechanism of olefin metathesis reactions catalyzed by **1** and its analogues has been the subject of intense experimental[4−6] and theoretical[7] investigation, with the ultimate goal of facilitating the rational design of new catalysts displaying superior activity, stability, and selectivity. Early mechanistic studies of the catalysts $(PR_3)_2(X)_2Ru{=}CHR^1$ established that phosphine dissociation is a critical step along the olefin metathesis reaction coordinate and demonstrated that catalysts containing sterically bulky and electron-donating phosphine ligands display the highest catalytic activity.[4a] This trend was explained on the basis of the increased trans-effect of larger and more basic phosphines, which was believed to accelerate dissociation of the second PR_3 ligand and to stabilize the Ru(IV) metallacyclobutane intermediate.[4a]

On the basis of these important studies, we[8] and others[9,10] have developed a new class of ruthenium alkylidenes containing N-heterocyclic carbene (NHC) ligands, which are significantly larger and more electron donating than trialkylphosphines.[11] The new complexes were prepared by substitution of a single PCy_3 ligand of **1** with an N-heterocyclic carbene to produce products of the general formula $(NHC)(PCy_3)(Cl)_2Ru{=}CHPh$. These "second generation" ruthenium olefin metathesis catalysts exhibit dramatically increased reactivity with olefinic substrates relative to that of the parent catalyst **1**. For example, in ring closing metathesis (RCM) and cross-metathesis (CM) reactions, NHC−ruthenium complexes catalyze the formation of tri- and tetrasubstituted olefins,[8,12,13] as well as functionalized alkenes[14] in good to excellent yields. The NHC complexes, particularly **8** and **14** (Figure 1), are also highly active catalysts for the ring opening metathesis polymerization of cyclooctadiene (COD).[15] In fact, the rate of COD polymerization catalyzed by **8** even surpasses that of electrophilic early transition metal-based catalyst systems.[16] The high activity of the NHC catalysts was originally attributed to increased labilization of the phosphine due to the large trans-effect of the NHC ligands.[8−10] However, in a preliminary communication, we reported the surprising result that phosphine dissociation in **8** is extremely slow relative to that in **1**.[6]

(1) Ivin, K. J.; Mol, J. C. *Olefin Metathesis and Metathesis Polymerization*; Academic Press: San Diego, CA, 1997.

(2) Schwab, P.; Grubbs, R. H.; Ziller, J. W. *J. Am. Chem. Soc.* **1996**, *118*, 100.

(3) For recent reviews in this area, see: (a) Trnka, T. M.; Grubbs, R. H. *Acc. Chem. Res.* **2001**, *34*, 18. (b) Furstner, A. *Angew. Chem., Int. Ed.* **2000**, *39*, 3012. (c) Grubbs, R. H.; Chang, S. *Tetrahedron* **1998**, *54*, 4413.

(4) (a) Dias, E. L.; Nguyen, S. T.; Grubbs, R. H. *J. Am. Chem. Soc.* **1997**, *119*, 3887. (b) Ulman, M.; Grubbs, R. H. *Organometallics* **1998**, *17*, 2484.

(5) (a) Adlhart, C.; Volland, M. A. O.; Hofmann, P.; Chen, P. *Helv. Chim. Acta* **2000**, *83*, 3306. (b) Adlhart, C.; Chen, P. *Helv. Chim. Acta* **2000**, *83*, 2192. (c) Adlhart, C.; Hinderling, C.; Baumann, H.; Chen, P. *J. Am. Chem. Soc.* **2000**, *122*, 8204. (d) Hinderling, C.; Adlhart, C.; Chen, P. *Angew. Chem., Int. Ed.* **1998**, *37*, 2685.

(6) Sanford, M. S.; Ulman, M.; Grubbs, R. H. *J. Am. Chem. Soc.* **2001**, *123*, 749.

(7) (a) Meier, R. J.; Aagaard, O. M.; Buda, F. *J. Mol. Catal. A* **2000**, *160*, 189. (b) Aagaard, O. M.; Meier, R. J.; Buda, F. *J. Am. Chem. Soc.* **1998**, *120*, 7174.

(8) (a) Morgan, J. P.; Grubbs, R. H. *Org. Lett.* **2000**, *2*, 3153. (b) Scholl, M.; Ding, S.; Lee, C. W.; Grubbs, R. H. *Org. Lett.* **1999**, *1*, 953. (c) Scholl, M.; Trnka, T. M.; Morgan, J. P.; Grubbs, R. H. *Tetrahedron Lett.* **1999**, *40*, 2247.

(9) Huang, J.; Stevens, E. D.; Nolan, S. P.; Peterson, J. L. *J. Am. Chem. Soc.* **1999**, *121*, 2674.

(10) Weskamp, T.; Kohl, F. J.; Hieringer, W.; Gliech, D.; Herrmann, W. A. *Angew. Chem., Int. Ed.* **1999**, *38*, 2416.

(11) (a) Herrmann, W. A.; Kocher, C. *Angew. Chem., Int. Ed. Engl.* **1997**, *36*, 2162. (b) Huang, J.; Schanz, H. J.; Stevens, E. D.; Nolan, S. P. *Organometallics* **1999**, *18*, 2370.

(12) Ackermann, L.; Furstner, A.; Weskamp, T.; Kohl, F. J.; Herrmann, W. A. *Tetrahedron Lett.* **1999**, *40*, 4787.

(13) Chatterjee, A. K.; Grubbs, R. H. *Org. Lett.* **1999**, *1*, 1751.

(14) (a) Choi, T. L.; Chatterjee, A. K.; Grubbs, R. H. *Angew. Chem, Int. Ed.* **2001**, *40*, 1277. (b) Chatterjee, A. K.; Morgan, J. P.; Scholl, M.; Grubbs, R. H. *J. Am. Chem. Soc.* **2000**, *122*, 3783.

(15) Bielawski, C. W.; Grubbs, R. H. *Angew. Chem., Int. Ed.* **2000**, *39*, 2903.

(16) (a) Schrock, R. R. *Polyhedron* **1995**, *14*, 3177. (b) Schrock, R. R. *Tetrahedron* **1999**, *55*, 8141.

10.1021/ja010624k CCC: $20.00
Published on Web 06/16/2001

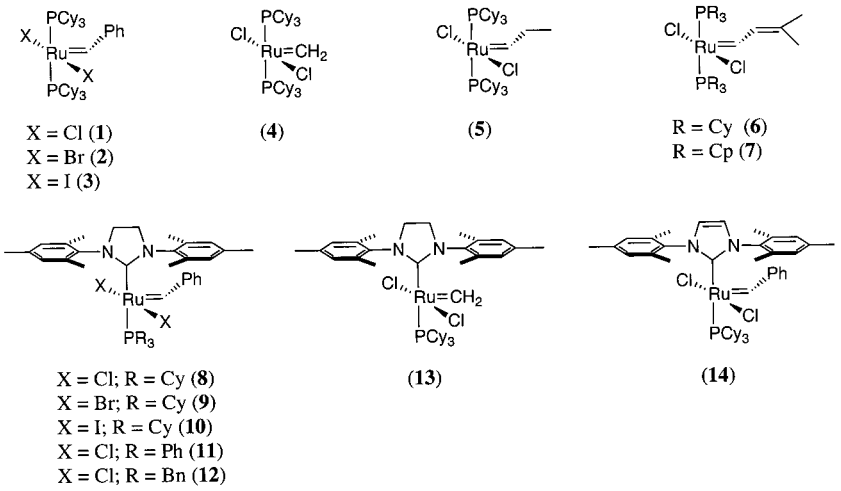

Figure 1. Catalysts **1**−**14**.

Scheme 1

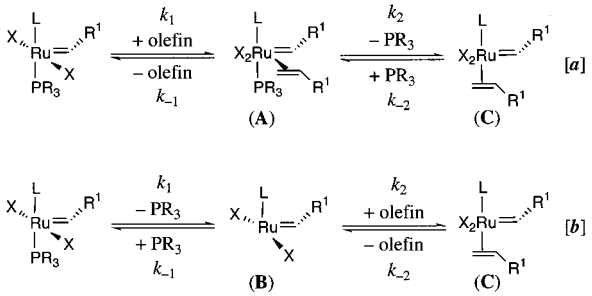

We describe herein an extensive and systematic evaluation of the effects of ligand variation on the kinetics and mechanism of ruthenium-catalyzed olefin metathesis reactions. A series of ruthenium complexes with the general formula $L(PR_3)(X)_2Ru{=}CHR^1$ have been examined, and the influence of the substituents L, X, R, and R^1 on the rate of phosphine exchange and on the kinetics of initiation and propagation in olefin metathesis reactions is described in detail. On the basis of these data, a detailed mechanism for ruthenium-based olefin metathesis catalysis is presented. Finally, the implications of these studies for the design and implementation of new catalysts and substrates are discussed.

Results

Phosphine Exchange. A series of ruthenium catalysts of the general formula $L(PR_3)(X)_2Ru{=}CHR^1$ (Figure 1) were prepared in order to probe the effect of each substituent (X, L, R, and R^1) on catalyst reactivity. The bis-phosphine complexes (**1**−**7**) and the NHC-coordinated complexes (**8**−**14**) represent the two major classes of ruthenium metathesis catalysts developed by our group over the past several years. Initial investigations of catalysts **1**−**14** were focused on the ligand exchange of phosphine with olefinic substrate (Scheme 1). An understanding of this initial ligand substitution is critical because this reaction allows entry of **1**−**14** into the olefin metathesis catalytic cycle. In the two limiting cases, this substitution could occur according to an associative (Scheme 1a) or a dissociative (Scheme 1b) pathway. In the former pathway, olefin coordination to form an 18-electron intermediate (or transition state) (**A**) is followed by dissociation of phosphine, while in the latter, phosphine dissociation to generate a 14-electron intermediate (**B**) is followed by trapping with the olefinic substrate. Early mechanistic studies (involving analogues of catalysts **1**−**3**)[17] could not distinguish between these two pathways, but an associative exchange was proposed on the basis of a preference for the 18-electron over the 14-electron intermediate.[4a] It has proven difficult to investigate this ligand displacement directly in solution because the putative ruthenium−olefin adduct (**C**) cannot be observed by spectroscopic methods.[18] As such, we undertook studies using the degenerate exchange of free and bound PR_3 (Scheme 2) as a simple, but potentially relevant, model system for the phosphine/olefin substitution.

Scheme 2

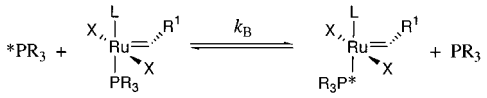

^{31}P NMR spectroscopy showed that phosphine exchange in catalysts **1**−**14** is relatively slow on the NMR time scale, and coalescence of the free and bound phosphine signals was not observed up to 80 °C in toluene-d_8.[19] Therefore, ^{31}P NMR magnetization transfer (MT) experiments were utilized to determine phosphine exchange rates in **1**−**14**. In these MT experiments, the free phosphine resonance was selectively inverted using a DANTE pulse sequence,[20] and ^{31}P NMR spectra were recorded after variable mixing times (ranging between 0.00003 and 50 s). The time-dependent magnetization data were analyzed using the computer program CIFIT,[21] and rate constants (k_B) for the exchange between bound and free phosphine were obtained for all of the catalysts. This analysis also provided T_1 values for both free and bound phosphine, and independent T_1 analysis showed good agreement with the calculated values.

As summarized in Table 1, the phosphine exchange rate constants (k_B) at 80 °C for ruthenium complexes **1**−**14** range over *6 orders of magnitude*! In fact, the rate constants at the high and low ends of the scale could not be measured by magnetization transfer at 80 °C and were obtained by extrapolation from Eyring plots. For the olefin metathesis catalysts

(17) The mechanistic studies detailed in ref 4a involved the diphenylvinyl carbene analogues of benzylidenes **1**−**3**.

(18) Chen and co-workers have provided mass spectrometric evidence that *dissociative* substitution of phosphine with olefinic substrates occurs in ruthenium catalyzed olefin metathesis reactions in the gas phase (ref 5).

(19) Even at 100 °C, only catalyst **3** shows significant line broadening. Higher temperatures were not accessible in these systems because catalyst decomposition was observed.

(20) Morris, G. A.; Freeman, R. *J. Magn. Reson.* **1978**, *29*, 433.

(21) Bain, A. D.; Kramer, J. A. *J. Magn. Reson.* **1996**, *118A*, 21.

Table 1. Rate Constants and Activation Parameters for Phosphine Exchange[a]

catalyst	k_B (s^{-1}) 80 °C[b]	$\Delta H^{\ddagger}$ (kcal/mol^{-1})	$\Delta S^{\ddagger}$ (eu)	$\Delta G^{\ddagger}$(298 K) (kcal/mol^{-1})
1	9.6 ± 0.2	23.6 ± 0.5	12 ± 2	19.88 ± 0.06
2	30 ± 2	23.1 ± 0.3	13 ± 1	19.11 ± 0.03
3	1660 ± 220[c]	19.0 ± 0.5	10 ± 2	16.12 ± 0.01
4[d]				
5	19.4 ± 0.8	24.3 ± 0.6	16 ± 2	19.6 ± 0.1
6	0.33 ± 0.02	24 ± 1	8 ± 3	22.0 ± 0.2
7	1.42 ± 0.06	24 ± 1	11 ± 3	21.1 ± 0.1
8	0.13 ± 0.01	27 ± 2	13 ± 6	23.0 ± 0.4
9	0.52 ± 0.02	27 ± 2	15 ± 6	22.0 ± 0.4
10	29 ± 3	23 ± 4	12 ± 11	19.0 ± 0.5
11	7.5 ± 0.5[c]	21 ± 3	5 ± 9	19.6 ± 0.3
12	0.165 ± 0.006	27 ± 1	13 ± 4	22.7 ± 0.3
13[d]				
14	0.03 ± 0.01[c]	25 ± 4	6 ± 11	24 ± 1

[a] Reactions were carried out in toluene-d_8 with 1 equiv of Ru ([Ru] = 0.04 M) and 1.5 equiv of free PR_3 (relative to bound PR_3). [b] Values for k_B are reported per coordinated PR_3 ligand. [c] Values for k_B at 80 °C were extrapolated from Eyring plots. [d] Values for k_B in complexes **4** and **13** could not be determined due to catalyst decomposition at the elevated temperatures required for these experiments.

$L(PR_3)(X)_2Ru{=}CHR^1$, all of the ligands X, L, R, and R^1 were found to have a significant influence on the rate of phosphine exchange. The most striking ligand effect in this series involves the two most widely used ruthenium-based olefin metathesis catalysts: $(PCy_3)_2(Cl)_2Ru{=}CHPh$ (**1**) and $(IMesH_2)(PCy_3)(Cl)_2Ru{=}CHPh$ (**8**) ($IMesH_2$ = 1,3-dimesityl-4,5-dihydroimidazol-2-ylidene). As we noted in our earlier communication,[6] the simple substitution of one PCy_3 ligand of **1** with an N-heterocyclic carbene ($IMesH_2$) results in a *decrease* in phosphine exchange rate of over 2 orders of magnitude.[22] The large difference in k_B is particularly notable because **8** exhibits much higher olefin metathesis activity than **1**[15] and the sterically bulky and highly basic $IMesH_2$ ligand was originally designed to accelerate the phosphine dissociation event.

More subtle changes of the phosphine and/or the N-heterocyclic carbene L-type ligands also have a significant impact on the rate of phosphine dissociation. For example, in the bis-phosphine complexes, substitution of tricyclohexyl- with tricyclopentylphosphine (catalysts **6** and **7**, respectively) leads to a 4-fold increase in k_B. The result is intriguing because PCy_3 and PCp_3 are believed to have very similar steric and electronic parameters.[23]

In the N-heterocyclic carbene-containing catalysts, replacing the $IMesH_2$ ligand (containing a saturated imidazolyl ring) with the IMes (IMes = 1,3-dimesitylimidazol-2-ylidene) ligand (containing an unsaturated imidazolyl ring) suppresses k_B by close to an order of magnitude (complexes **8** and **14**, respectively). In addition, substitution of the PCy_3 ligand of **8** with PPh_3 (**11**) leads to a 50-fold increase in the rate of phosphine exchange. However, when the PCy_3 of **8** is replaced with PBn_3 (**12**) (a phosphine with steric and electronic properties that are intermediate between PPh_3 and PCy_3),[24] only a very small increase in k_B is observed.

Substitution of the X-type ligands also has a large influence on k_B. As X is changed from chloride to bromide to iodide (catalysts **1**, **2**, and **3**, respectively), the phosphine exchange rate increases by 2 orders of magnitude. The increase in k_B between **1** and **2** (a factor of about 3) is much less than that between **2** and **3** (a factor of approximately 55). The phosphine exchange rate in the di-iodide catalyst, $(PCy_3)_2(I)_2Ru{=}CHPh$ (**3**) (1660 s^{-1} at 80 °C), is the largest observed for any ruthenium complex in this study. Halide substitution in the $IMesH_2$-ligated complexes (catalysts **8**, **9**, and **10**) shows almost identical trends in k_B as in the bis-phosphine series, and the di-iodide catalyst $(IMesH_2)(PCy_3)(I)_2Ru{=}CHPh$ (**10**) exchanges phosphine almost 225 times faster than the di-chloride complex **8**. Notably, olefin metathesis activity in catalysts **1**−**3** is *inversely proportional* to k_B. [The relative rates (k_{rel}) for the RCM of diethyl diallylmalonate have been reported as approximately 20 (catalyst **1**), 15 (catalyst **2**), and 1 (catalyst **3**).[4a,17]]

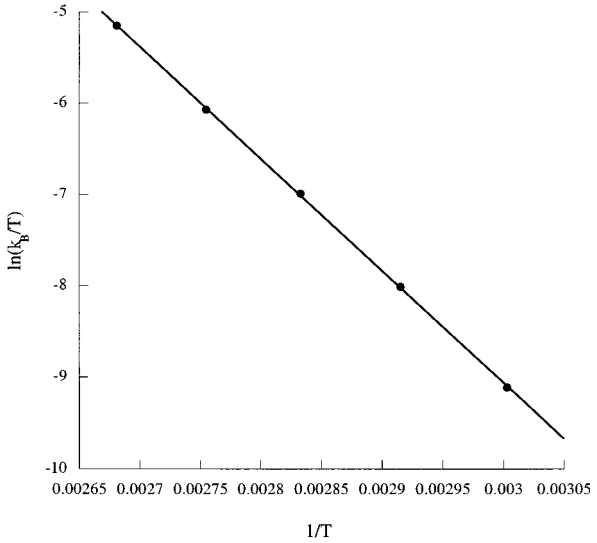

Figure 2. Eyring plot for phosphine exchange in catalyst **6**.

Finally, the nature of the substituent (R^1) on the carbene α-carbon also affects the dynamics of phosphine exchange. The magnitude of k_B for $R^1 = CH_3CH_2$ (**5**) > Ph (**1**) > $CHCHC(CH_3)_2$ (**6**) ≫ H (**4**). In fact, the value of k_B for the methylidene complexes $(PCy_3)_2(Cl)_2Ru{=}CH_2$ (**4**) and $(IMesH_2)(PCy_3)(Cl)_2Ru{=}CH_2$ (**13**) could not even be measured using this technique because of catalyst instability at the temperatures required for magnetization transfer experiments.

Examination of the rate constant (k_B) as a function of phosphine concentration established a dissociative mechanism for this degenerate exchange reaction. For all of the catalysts **1**−**14**, k_B was independent (within error) of [PR_3] over a wide range of phosphine concentrations (0.04−0.77 M). Activation parameters for phosphine dissociation in each complex were obtained from Eyring plots, and the results are summarized in Table 1. In addition, a representative Eyring plot (for complex **6**) is shown in Figure 2. The activation entropies ($\Delta S^{\ddagger}$) in these systems are all positive in sign and range between 5 and 16 eu. Typically, $\Delta S^{\ddagger}$'s above 10 eu indicate a dissociative reaction mechanism.[25] The values of $\Delta H^{\ddagger}$ in catalysts **1**−**14** are all relatively large (>19 kcal/mol) and positive in sign. Although less diagnostic, these enthalpies of activation are also consistent with dissociative ligand exchange.[25] Interestingly, our experimental values for $\Delta H^{\ddagger}$ in catalysts **1** (23.6 ± 0.5 kcal/mol) and **14** (25 ± 4 kcal/mol) are in excellent agreement with ligand dissociation energies (ΔE) calculated by Herrmann for related model compounds (ΔE in $(PMe_3)_2(Cl)_2Ru{=}CH_2$ and (NHC)-

(22) The values of k_B are reported per coordinated phosphine ligand. As such, the phosphine exchange rate in solution for the bis−phosphine complexes **1**−**7** is actually double the values reported in Table 1.

(23) Cole, M. L.; Hibbs, D. E.; Jones, C.; Smithies, N. A. *J. Chem. Soc., Dalton Trans.* **2000**, 545.

(24) Tolman, C. A. *Chem. Rev.* **1977**, *77*, 313.

(25) Atwood, J. D. *Inorganic and Organometallic Reaction Mechanisms*; VCH: New York, 1997; p 13.

Scheme 3

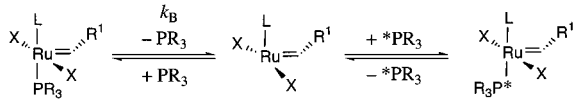

Scheme 4

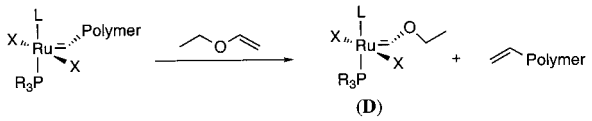

(**D**)

$(PMe_3)(Cl)_2Ru{=}CH_2$ (NHC = 1,3-dihydroimidazol-2-ylidene) were calculated to be 25.8 and 24.9 kcal/mol respectively).[10]

The magnetization transfer data described above suggest that phosphine substitution in complexes **1**−**14** proceeds by a dissociative mechanism. As summarized in Scheme 3, this mechanism involves initial phosphine dissociation to produce a four-coordinate, 14-electron intermediate $L(X)_2Ru{=}CHR^1$ (**B**). This intermediate has not been observed by ^{31}P or ^1H NMR spectroscopy, indicating that the equilibrium for phosphine dissociation lies very far toward the 16-electron starting material in these systems. In the degenerate exchange, this 14-electron intermediate undergoes rapid trapping by free PR_3 to regenerate the starting complex. Importantly, recent results have shown that four-coordinate ruthenium carbenes similar to the proposed intermediate **B** can be stable under certain conditions.[18,26]

Initiation Kinetics. The phosphine exchange rates observed for complexes **1**−**14** are clearly not directly proportional to their olefin metathesis activities. [In fact, if anything, an approximately inverse relationship between olefin metathesis activity and k_B is observed.] As such, we considered that k_B might, instead, be related to the initiation rates of these catalysts. The initiation event involves the initial substitution of phosphine with olefinic substrate, which allows entry of the "dormant" species **1**−**14** into the olefin metathesis catalytic cycle. The kinetics of initiation can be measured by monitoring the stoichiometric reaction of a ruthenium complex with a judiciously chosen olefin, ethyl vinyl ether. The reaction of ruthenium carbenes with ethyl vinyl ether has been utilized as a method for quenching ring opening metathesis polymerizations.[27] This reaction is highly regioselective and results in the quantitative formation of a Fischer carbene complex (**D**) and an olefin-capped polymer chain (Scheme 4). Ethyl vinyl ether offers the advantages that it reacts rapidly, quantitatively, and irreversibly with all of the catalysts under investigation.[28] As a result, these reactions generally proceed with clean kinetics and provide close to an upper limit for the initiation rates of catalysts **1**−**14**.[29]

Under saturation conditions, the initiation kinetics of catalysts **1**−**14** may be related to the rates of phosphine exchange in these systems. As shown in Scheme 1b, dissociative substitution of phosphine with olefinic substrate proceeds through the four-coordinate intermediate **B**. Application of the steady-state approximation to **B** affords the rate expression shown in eq 1. Under conditions where $k_{-1}[PR_3] \ll k_2[\text{olefin}]$ (saturation), this expression is reduced to eq 2, and phosphine dissociation becomes the rate-determining step of the reaction. As described above, the rate constant for phosphine dissociation ($k_1 = k_B$) has already been determined for catalysts **1**−**14**.

$$\text{rate} = k_1k_2[\text{Ru}][\text{olefin}]/\{k_{-1}[PR_3] + k_2[\text{olefin}]\} \quad (1)$$

$$\text{rate} = k_1[\text{Ru}] \text{ when } (k_{-1}[PR_3] \ll k_2[\text{olefin}]) \quad (2)$$

Initiation Kinetics by NMR Spectroscopy. The reactions of catalysts **1**−**14** with ethyl vinyl ether were studied by ^1H NMR spectroscopy using a large excess of olefin (15−60 equiv relative to [Ru]). The disappearance of the starting catalyst (0.017 M in toluene-d_8) was monitored as a function of time, and unless otherwise noted, the reactions showed clean first-order kinetics over at least 3 half-lives. Initial investigations focused on the reactivity of the NHC-coordinated complexes **8**−**12** and **14**. For all of these catalysts, the initiation rate constant (k_{Init}) was *completely independent* of olefin concentration over a concentration range of 0.173 to 1.02 M. Additionally, k_{Init} was insensitive to the structure of the vinyl ether substrate. For example, the values of k_{Init} for the reaction of **8** with ethyl vinyl ether, ethyl 1-propenyl ether, 2,3-dihydrofuran, and 3,4-dihydropyran[30] were identical within the error of the measurements (in each case, $k_{Init} = (4.6 \pm 0.4) \times 10^{-4}$ s^{-1} at 35 °C). These results demonstrate that saturation conditions (eq 2) are achieved even at relatively low concentrations of olefinic substrate and suggest that phosphine dissociation is the rate-determining step of these reactions. This can be confirmed by comparison of the k_{Init} values with the phosphine dissociation rates (k_B) of these catalysts. (Values of k_B were extrapolated to the appropriate temperature from the Eyring plots of the magnetization transfer data.) As shown in Table 2, k_{Init} and k_B are identical (within error) for each of the catalysts **8**−**12** and **14**.

The methylidene complex **13** was a notable anomaly in the NHC-coordinated catalyst systems. Extremely high temperatures (>80 °C) were required in order to observe appreciable reaction of **13** with ethyl vinyl ether, implying that phosphine dissociation from this complex is extremely slow. In fact, under these forcing reaction conditions, the decomposition of **13** occurred on the same time scale as the initiation event, and as such, only an upper limit for k_{Init} could be established for this complex ($k_{Init} \leq 1 \times 10^{-3}$ s^{-1} at 85 °C).

Several of the bis-phosphine catalysts showed saturation kinetics by ^1H NMR spectroscopy. The initiation rate constants (k_{Init}) for the reactions of complexes **4** and **6** with ethyl vinyl ether were found to be independent of olefin concentration

(26) (a) Sanford, M. S.; Henling, L. M.; Day, M. W.; Grubbs, R. H. *Angew. Chem., Int. Ed.* **2000**, *39*, 3451. (b) Coalter, J. N.; Bollinger, J. C.; Eisenstein, O.; Caulton, K. G. *New J. Chem.* **2000**, *24*, 925.

(27) For a recent example, see: Maynard, H. D.; Okada, S. Y.; Grubbs, R. H. *Macromolecules* **2000**, *33*, 6239.

(28) Fischer carbene complexes can be active for olefin metathesis reactions under some conditions (see references below). However, throughout the kinetics experiments described herein, Fischer carbene formation is quantitative and irreversible by ^1H NMR spectroscopy. (a) Katayama, H.; Urushima, H.; Nishioka, T.; Wada, C.; Nagao, M.; Ozawa, F. *Angew. Chem., Int. Ed.* **2000**, *39*, 4513. (b) van der Schaaf, P. A.; Kolly, R.; Kirner, H. J.; Rime, F.; Muhlebach, A.; Hafner, A. *J. Organomet. Chem.* **2000**, *606*, 65. (c) Katayama, H.; Urushima, H.; Ozawa, F. *J. Organomet. Chem.* **2000**, *611*, 332.

(29) Previously, initiation studies of catalysts **1**−**14** utilized terminal olefinic substrates such as 1-hexene (refs 2 and 4b) or 1-butene (ref 5c). However, unlike the reaction with ethyl vinyl ether, these reactions are readily reversible and lead to the formation of both kinetic (alkylidene) and thermodynamic (methylidene) products. Particularly in the case of the NHC-containing catalysts **8**−**14**, the simultaneous formation of alkylidene and methylidene products leads to complications in the kinetic analysis.

(30) The reaction of 3,4-dihydropyran is particularly significant because it involves the ring opening a relatively low strained six-membered ring. This is typically a challenge for olefin metathesis catalysts (the ring opening of cyclohexene, for example, is only effected by extremely thermodynamically unstable carbenes) and speaks to the favorable thermodynamics associated with the generation of Fischer carbene moieties. Ulman, M.; Belderrain, T. R.; Grubbs, R. H. *Tetrahedron Lett.* **2000**, *41*, 4689.

Table 2. ^{1}H NMR Initiation Kinetics[a]

catalyst	T (°C)	k_{Init} (s^{-1})	k_B(predicted) (s^{-1})[b]
1	10	$(1.0 \pm 0.1) \times 10^{-3}$	$(3.8 \pm 0.6) \times 10^{-3}$
2	0	$(1.1 \pm 0.1) \times 10^{-3}$	$(3.1 \pm 0.4) \times 10^{-3}$
3[c]	5	$(2.4 \pm 0.4) \times 10^{-3}$	1.7 ± 0.1
4	40	$(8.5 \pm 0.3) \times 10^{-4}$	
5	0	$(5.4 \pm 0.5) \times 10^{-4}$	$(1.1 \pm 0.2) \times 10^{-3}$
6	25	$(1.0 \pm 0.1) \times 10^{-3}$	$(9 \pm 3) \times 10^{-4}$
7	25	$(1.5 \pm 0.3) \times 10^{-3}$	$(4.0 \pm 0.8) \times 10^{-3}$
8	35	$(4.6 \pm 0.4) \times 10^{-4}$	$(4 \pm 3) \times 10^{-4}$
9	35	$(2.0 \pm 0.1) \times 10^{-3}$	$(1.8 \pm 0.8) \times 10^{-3}$
10	0	$(2.8 \pm 0.2) \times 10^{-3}$	$(2 \pm 1) \times 10^{-3}$
11	10	$(3.3 \pm 0.2) \times 10^{-3}$	$(4 \pm 2) \times 10^{-3}$
12	50	$(5.4 \pm 0.5) \times 10^{-3}$	$(4 \pm 1) \times 10^{-3}$
13[c]	85	$\leq 1 \times 10^{-3}$	
14	50	$(5 \pm 2) \times 10^{-4}$	$(1.0 \pm 0.6) \times 10^{-3}$

[a] Reactions were carried out in toluene-d_8, [Ru] = 0.017 M and [olefin] = 0.50 M (30 equiv). [b] k_B(predicted) was determined by extrapolation of Eyring plots from the magnetization transfer data to the temperature of the initiation experiment for each catalyst. [c] Complexes **3** and **13** did not show clean first-order kinetics.

([olefin] = 0.173−1.02 M). Furthermore, k_{Init} in these systems showed excellent agreement with the predicted values of k_B (Table 2). These data indicates that, in **4** and **6**, phosphine dissociation is the slow step of the reaction sequence. Notably, the bis-phosphine methylidene **4** initiated quite slowly relative to the other bis-phosphine catalysts (Table 2). However, initiation in catalyst **4** ($k_{Init} = 8.5 \times 10^{-4}$ s^{-1} at 40 °C) was still significantly more efficient than in the NHC methylidene **13**, and methylidene decomposition was not competitive with initiation at 40 °C in this system.

NMR initiation kinetics of the bis-phosphine catalysts **1**, **2**, **3**, **5**, and **7** showed an approximately linear dependence on olefin concentration. In these complexes, k_B is large (for **1**, **2**, **3**, **5**, and **7**, $k_B > 1$ s^{-1} at 80 °C), and phosphine dissociation is not rate determining at low concentrations of olefin. In fact, even up to the highest concentrations accessible by NMR spectroscopy (approximately 120 equiv of ethyl vinyl ether relative to [Ru]), k_{Init} remained strongly dependent on [olefin]. Importantly, these NMR experiments are still consistent with a dissociative mechanism, since the values obtained for k_{Init} are well below those predicted by magnetization transfer for saturation conditions (Table 2).

Initiation Kinetics by UV−Vis Spectroscopy. Since saturation could not be achieved by ^{1}H NMR spectroscopy, we studied initiation kinetics in catalysts **1**, **2**, **3**, **5**, and **7** by UV−vis spectroscopy. The reaction of these ruthenium complexes with ethyl vinyl ether was accompanied by a color change from purple/red to orange and a corresponding blue shift of the visible absorbance. This relatively weak band (extinction coefficients typically range from 700 to 1500 dm^3 mol^{-1} cm^{-1}) is likely due to metal to ligand charge transfer (MLCT) into the π^* orbital of the Ru=CHR[1] bond.[31] The MLCT band provides an excellent handle for following both the disappearance of starting material and the appearance of product. The reactions of catalysts **1**, **2**, **4**, and **7** (0.77 mM in toluene) with ethyl vinyl ether were each monitored at an appropriate wavelength (of the product), and the kinetics data showed clean first-order fits over 5 half-lives.[32] For each complex, the initiation rate constant was determined as a function of ethyl vinyl ether concentration ([ethyl vinyl ether] = 0.024 to 1−3 M), and a representative plot of k_{Init} vs [olefin] (for complex **1**) is shown in Figure 3. As expected for a dissociative substitution, k_{Init} becomes independent of [ethyl vinyl ether] at high concentrations where k_2[olefin] becomes much greater than k_{-1}[PR_3]. Most importantly, the values obtained for k_{Init} at saturation were identical to the predicted k_B's, within the error of the two measurements (Table 3). The UV−vis data as well as the ^{1}H NMR studies described above confirm that dissociative substitution of phosphine for olefinic substrate (Scheme 1b) is the operative initiation pathway in all of the catalysts **1**−**14**.

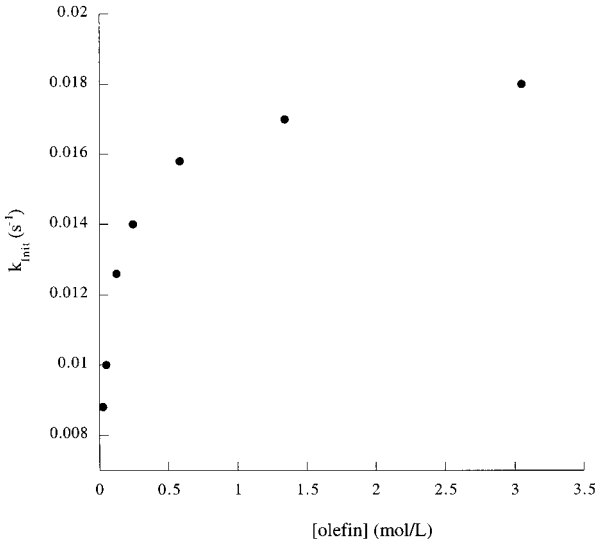

Figure 3. k_{Init} vs [olefin] for catalyst **1**.

Table 3. UV−vis Initiation Kinetics[a]

complex	T (°C)	wavelength (nm)	k_{Init}(saturation) (s^{-1})	k_B(predicted) (s^{-1})
1	20	484	0.016 ± 0.001	0.016 ± 0.002
2	20	486	0.057 ± 0.002	0.060 ± 0.005
5	20	354	0.028 ± 0.002	0.026 ± 0.003
7	30	468	0.074 ± 0.002	0.079 ± 0.003

[a] Reactions carried out in toluene; [Ru] = 0.77 mM and [olefin] = 0.58 M.

Table 4. Solvent Effects on Initiation

catalyst	solvent	dielectric constant (ϵ)	k_{Init} (s^{-1})
1[a]	pentane	1.84	0.013 ± 0.001
1[a]	toluene	2.38	0.016 ± 0.001
1[a]	diethyl ether	4.34	0.022 ± 0.004
1[a]	CH_2Cl_2	8.9	0.021 ± 0.001
1[a]	THF	7.32	0.032 ± 0.004
8[b]	toluene-d_8	2.38	$(4.6 \pm 0.4) \times 10^{-4}$
8[b]	CD_2Cl_2	8.9	$(6.1 \pm 0.2) \times 10^{-4}$
8[b]	THF-d_8	7.32	$(1.0 \pm 0.1) \times 10^{-3}$

[a] Reactions kinetics measured by UV−vis spectroscopy (484 nm) at 20 °C with [Ru] = 0.77 mM and [olefin] = 0.58 M. [b] Reaction kinetics measured by ^{1}H NMR spectroscopy at 35 °C with [Ru] = 0.017 M and [olefin] = 0.50 M.

Solvent Effects on Initiation. Changes of solvent were found to have a significant impact on the initiation rates of catalysts **1**−**14**. A systematic examination of catalyst initiation as a function of solvent was carried out using complexes **1** (by UV−vis spectroscopy) and **8** (by ^{1}H NMR spectroscopy). As summarized in Table 4, k_{Init} was found to be roughly proportional to the dielectric constant of the reaction medium. For both catalysts, the initiation rate increased by 30% upon

(31) This assignment is consistent with Hofmann's calculations which suggest that the LUMO of catalyst **1** (and its analogues) is localized primarily on C_α. Hansen, S. M.; Rominger, F.; Metz, M.; Hofmann, P. *Chem. Eur. J.* **1999**, *2*, 557.

(32) The reaction of **3** with ethyl vinyl ether showed anomalous UV−vis and NMR kinetics data, and quantitative measurement of the initiation rate of this complex was not possible. However, the value of k_{Init} for **3** was qualitatively much faster than that of the other four catalysts.

moving from toluene ($\epsilon = 2.38$) to dichloromethane ($\epsilon = 8.9$).[33] Both the magnitude and direction of this solvent effect are typical of dissociative ligand substitution reactions. For example, recent studies of dissociative exchange at neutral Pt(II) centers showed a 3-fold increase in rate constant upon moving from toluene to CH_2Cl_2.[34] The rate acceleration is these systems is likely the result of increased stabilization of the 4-coordinate intermediate **B** and/or of free PCy_3, since both are expected to be more polar than the ruthenium starting material. The stabilization of **B** may involve coordination of solvent to the electron-deficient Ru(II) center (particularly in the case of THF and diethyl ether); however no evidence of solvento adducts has been detected by ^{1}H or ^{31}P NMR spectroscopy. These solvent effects are particularly significant in light of recent gas-phase mass spectrometric investigations of ruthenium olefin metathesis reactions.[5] While these studies provide extremely valuable information that cannot be obtained through solution studies, they do not take into account solvent interactions which may be critical, particularly when highly polar and/or charged intermediates are involved.

Estimation of k_{-1}/k_2. As summarized in Scheme 1b, the dissociative reactions of ruthenium complexes **1**−**14** with olefinic substrates are governed by two important factors. The first factor is the rate of phosphine dissociation [$k_1 = k_B = k_{Init}$ (saturation)] to produce the 14-electron intermediate **B**, and a second consideration is the reactivity of this intermediate. Complex **B** can be trapped by free PR_3 to regenerate the 16-electron starting material (at a rate proportional to k_{-1}) or it can bind olefinic substrate and undergo productive olefin metathesis reactions (at a rate proportional to k_2). An estimate of the ratio of these two rate constants (k_{-1}/k_2) can be obtained by manipulation of eq 1. In the presence of a large excess of olefin and of free PR_3, a linear relationship between $1/k_{obs}$ and [PR_3]/[olefin] (eq 3) is obtained.

$$1/k_{obs} = k_{-1}[PR_3]/k_1k_2[\text{olefin}] + 1/k_1 \qquad (3)$$

Notably, two important assumptions were made in the derivation of eq 3. First, this equation requires that olefin coordination is essentially irreversible ($k_2 \gg k_{-2}$). This is obviously somewhat unrealistic since the reversibility of this step is crucial to achieving catalytic turnover in olefin metathesis reactions. However, the use of ethyl vinyl ether (which undergoes a single, irreversible olefin metathesis event with **1**−**14**)[28] should improve the validity of the assumption in these systems. A second approximation inherent to this derivation is that all of the steps after olefin coordination (particularly metallacylobutane formation) are fast. This is likely a better assumption for the NHC-containing complexes (**8**−**14**) than for the bis-phosphine adducts (**1**−**7**). The former contain highly electron donating N-heterocyclic carbene ligands which are expected to better stabilize high oxidation state ruthenium intermediates. In systems where this approximation is not good, k_{-1}/k_2 is likely to be overestimated since additional k_3 and k_{-2} terms are not included. However, despite these caveats, we feel that eq 3 provides a very simple and useful starting point for understanding the olefin metathesis reactivity of catalysts **1**−**14**.

^{1}H NMR kinetics of the reactions of the ruthenium complexes (0.017 mM in toluene-d_8) with ethyl vinyl ether were utilized to determine $1/k_{obs}$ as a function of [PR_3]/[olefin]. Both the concentration of PR_3 and the concentration of ethyl vinyl ether were varied, and the data showed the expected linear correlations for all of the catalysts investigated. The values obtained for k_1 [1/(intercept) of the linear curve fit] were generally close to k_B (predicted from the magnetization experiments). These values (which are summarized in Table S3) provide a third *independent* verification of k_1 and further confirm that a dissociative mechanism is operating in these systems.

Table 5. Values for the k_{-1}/k_2 Ratio for Selected Catalysts[a]

catalyst	T (°C)	k_{-1}/k_2
1	50	1.3×10^4
2	50	8.2×10^4
3	50	2.6×10^6
6	50	8.1×10^2
8	50	1.25
10	50	3.3×10^2
11	25	2.3
12	50	2.2

[a] Reaction kinetics measured by ^{1}H NMR spectroscopy with [Ru] = 0.017 M in toluene-d_8.

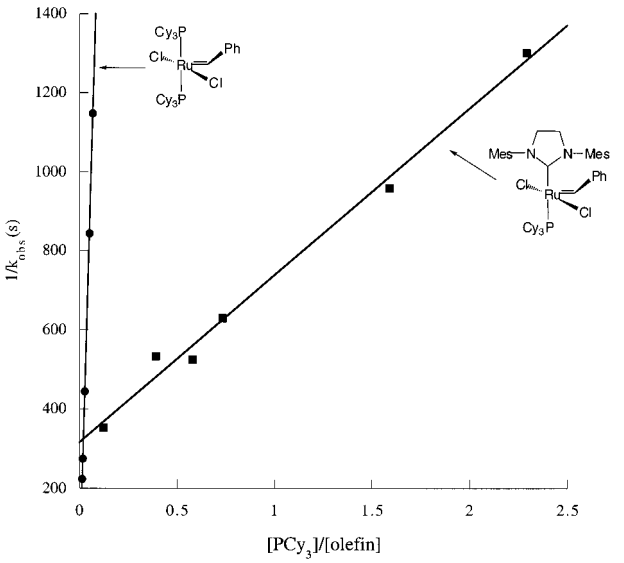

Figure 4. $1/k_{obs}$ vs [PCy_3]/[olefin] for catalysts **1** and **8**.

The bis-phosphine complexes **1**, **2**, **3**, and **6** as well as the $IMesH_2$ catalysts **8**, **10**, **11**, and **12** were investigated in this study, and k_{-1}/k_2 for each complex is listed in Table 5. A comparison of compounds **1** and **8** is indicative of the dramatic differences between the two series of catalysts, and an overlayed plot of $1/k_{obs}$ vs [PCy_3]/[olefin] for **1** and **8** is shown in Figure 4. At 50 °C, k_{-1}/k_2 is 1.3×10^4 for complex **1** and 1.25 for complex **8**. The decrease of *4 orders of magnitude* in k_{-1}/k_2 between **1** and **8** reflects a large (and general) increased selectivity for **8** to bind olefinic substrates in preference to PR_3. In both catalyst series, substitution of chloride with iodide results in a 100-fold increase in the k_{-1} to k_2 ratio. However, the relative difference in k_{-1}/k_2 for catalysts **3** and **10** remains 4 orders of magnitude. Also notable are the differences in k_{-1}/k_2 between **2** (8.2×10^4) and **10** (3.3×10^2). These catalysts dissociate phosphine at similar rates, and yet their k_{-1} to k_2 ratios differ by 2 orders of magnitude. A final comparison can be made between the $IMesH_2$ benzylidenes **8** and **11**, which contain PCy_3 and PPh_3, respectively. The magnitude of k_2 is identical in these two catalysts, since they both produce the same intermediate—$IMesH_{(2)}(Cl)_2Ru{=}CHPh$—upon dissociation of phosphine. As such, the values of k_{-1}/k_2 for **8** and **11** reflect the relative affinity of this intermediate for binding PCy_3 versus PPh_3. However, as shown in Table 5, these reactions were carried out at

(33) Gordon, A. J.; Ford, R. A. *The Chemists Companion*; John Wiley and Sons: New York, 1972; p 2.

(34) Plutino, M. R.; Scolaro, L. M.; Romeo, R.; Grassi, A. *Inorg. Chem.* **2000**, *39*, 2712.

substantially different temperatures (due to the extremely high reactivity of **11**), so these values can only be compared qualitatively.[35] It is important to point out that ethyl vinyl ether is an electron-rich olefin and reacts extremely rapidly with all of the catalysts **1**−**14**. Therefore, the data in Table 5 represent close to the lower limit of k_{-1}/k_2 for these systems. Nevertheless, we anticipate that the *relative* differences between these values for the catalysts should remain constant across a range of olefinic substrates.

Relative Catalyst Activities. The ring opening metathesis polymerization of cyclooctadiene has been studied using the new NHC catalysts **8**, **9**, **10**, **11**, and **13**. This reaction is frequently utilized as a standard for comparing the "activities" of single-component olefin metathesis catalysts.[10,15,36] In these systems, the rate of polymerization reflects the efficiency of both the initiation and the propagation steps of the metathesis reaction. As a result, the relative contributions of initiation and propagation to the overall activity of the catalysts can be difficult to deconvolute. Furthermore, the presence of multiple catalytically active species throughout a given polymerization[37] often precludes a simple kinetic analysis of the data. However, this reaction still serves as a useful benchmark for comparing the *relative activities* of our new ruthenium complexes. The ROMP of cyclooctadiene catalyzed by **8**, **9**, **10**, **11**, and **13** was carried out at 20 °C in CD_2Cl_2, and the reactions were monitored by ^{1}H NMR spectroscopy. In all cases, the disappearance of product was monitored over at least 3 half-lives, and the data were fitted to a first-order exponential. Although the first-order fits were not excellent for all of the catalysts, this treatment of the data has been shown to provide a good approximation of the lower limit of metathesis activity in related systems.[10,38]

The di-iodide catalyst **10** shows a slightly higher rate of polymerization than the di-chloride complex **8** (k_{rel} = 1 for **8** and 1.4 for **10**). The small increase in rate does not directly correlate with the amount of catalytically active species formed, since **10** initiates almost quantitatively (as determined by the nearly complete conversion of starting benzylidene to a new alkylidene), while initiation of **8** is highly inefficient. This indicates that the propagating species formed upon phosphine dissociation from **10** is significantly less active for metathesis than the propagating species from **8**. This result is consistent with earlier studies of metathesis activity in the di-chloride and di-iodide bis-phosphine catalysts **1** and **3**.[4a,17] Catalyst **9** has an initiation rate intermediate between those of **8** and **10** and is also expected to have an intermediate propagation rate. It is therefore noteworthy that **9** shows the same activity as **10** for COD polymerization (k_{rel} = 1.4), presumably due to the competing effects of initiation and propagation.

Of further interest is a comparison of the relative activities of **8** and **11**. Complexes **8** and **11** dissociate PR_3 to generate the same propagating species, so the rates of propagation in these two catalysts should be identical. However, catalyst **11** initiates more than 50 times faster than **8** and is therefore expected to be an exceptionally fast olefin metathesis catalyst. Under the same conditions used to measure the reaction rate of **8**, the polymerization of COD catalyzed by **11** is complete within seconds of adding monomer. In fact, the loading of catalyst **11** must be reduced 50-fold (relative to that of **8**) in order to achieve similar rates of polymerization. These results demonstrate that, with the appropriate choice of catalyst, highly efficient polymerizations can be achieved at significantly lower catalyst concentrations.[39] In contrast, methylidene **13** reacts exceptionally slowly with cyclooctadiene, and the relative rate of polymerization with this catalyst is over *4 orders of magnitude lower* than that of catalyst **8**. This is a particularly significant observation because this complex is a crucial intermediate during ring closing and cross-metathesis reactions of terminal olefins. The initiation studies described above suggest that this result is due, in large part, to the slow rate of phosphine dissociation in catalyst **13**.

Scheme 5

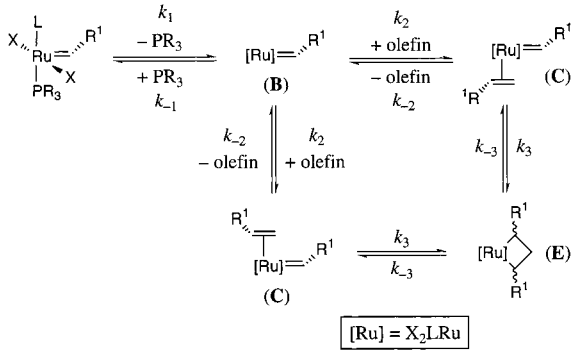

Discussion

Mechanism of Ruthenium-Catalyzed Olefin Metathesis Reactions. On the basis of the above data, we propose a general mechanism for olefin metathesis reactions catalyzed by **1**−**14**. As summarized in Scheme 5,[40] substitution of phosphine with olefinic substrate occurs in a dissociative fashion, to generate the four-coordinate intermediate **B**. Importantly, our results provide *no* evidence that an associative reaction pathway (involving the 18-electron olefin adduct **A**) contributes significantly to the metathesis reactions of any of these catalysts.[4a] In the bis-phosphine systems (complexes **1**−**7**), the 14-electron intermediate **B** is formed frequently (k_1 is large). However, under our reaction conditions, the recoordination of free PR_3 is competitive with substrate binding ($k_{-1}/k_2 \gg 1$). The active species carries out few catalytic turnovers before being "quenched" with free PR_3. In contrast, the NHC complexes (**8**−**14**) dissociate phosphine relatively inefficiently (k_1 is small). However, once the phosphine comes off, coordination of olefin is facile compared to re-binding of PR_3 ($k_{-1}/k_2 \sim 1$ and [olefin] is high). As such, the NHC complexes can perform multiple olefin metathesis events before they recoordinate phosphine and return to their resting state.

Notably, the catalytic cycle shown in Scheme 5 does not indicate stereochemistry about the ruthenium center for the important catalytic intermediates **C** and **E**. Several possibilities for the geometries of **C** and **E** have been proposed by our group[4a] and by Chen and co-workers.[5] However, the current work provides no evidence to support or refute either of these

(35) We feel that a reasonable comparison can be made in these systems because k_{-1}/k_2 is a ratio of second-order rate constants. As such, the temperature dependence of k_{-1} and k_2 should be roughly equivalent.

(36) Weskamp, T.; Schattenmann, W. C.; Spiegler, M.; Herrmann, W. A. *Angew. Chem., Int. Ed.* **1998**, *37*, 2490.

(37) The catalytically active species in these reaction mixtures include the un-initiated pre-catalyst and multiple ruthenium alkylidenes with appended polymer chains. Each of these complexes can initiate and propagate at different rates.

(38) Dias, E. L.; Grubbs, R. H. *Organometallics* **1998**, *17*, 2758.

(39) Notably, catalyst **11** carries out the RCM of terminal olefinic substrates with less than a 2-fold increase in rate relative to **8**. This appears to be due to competitive inhibition of the RCM reaction by ethylene generated as a consequence of the ring closing reaction.

(40) Scheme 5 outlines a generic *degenerate* olefin metathesis reaction (i.e., the ruthenium starting material and product are the same).

possibilities.[41] Another mechanistic question which remains concerns the possibility that metallacyclobutane (**E**) is a transition state rather than an intermediate along the olefin metathesis reaction coordinate.[5] Once again, this question cannot be answered definitively on the basis of the investigations described herein.

Ligand Effects on Olefin Metathesis Reactions. Although olefin metathesis reactions catalyzed by the complexes $L(PR_3)(X)_2Ru{=}CHR$[1] proceed according to the same general mechanistic pathway, the ancillary ligands play a significant role in determining the relative rates of the individual steps along the reaction coordinate.

(1) L-Type Ligand. The most important ligand effect in these systems involves the huge increase in olefin metathesis activity upon changing the L ligand from a phosphine to an N-heterocyclic carbene (e.g., catalysts **1** and **8**, respectively). The high activity of **8** relative to **1** can be understood on the basis of the k_{-1} to k_2 ratios of these two catalysts, which show that the $IMesH_2$ ligand increases selectivity for binding olefinic substrates over free phosphine by *4 orders of magnitude*. This improved selectivity may be explained by the electronic properties of NHC's, which are known to be excellent donor ligands relative to trialkylphosphines.[11,42,43] Cavell and coworkers have compared a series of Pd(0)−olefin complexes containing either N-heterocyclic carbenes or phosphines as ancillary ligands.[44] ^1H and ^{13}C NMR as well as IR spectroscopic studies indicate that the electron-donating NHC's promote and stabilize metal-to-olefin back-bonding to a much greater extent than the phosphine ligands in these systems.[44] Cavell's study is consistent with our observations that the NHC-coordinated complexes **8**−**14** show increased affinities for π-acidic olefinic substrates relative to σ-donating PR_3. Additionally, the $IMesH_2$ catalyst, **8**, is much more active for the polymerization of COD than the IMes complex **14**,[15] and the $IMesH_2$ ligand is a better electron donor than IMes.[11] Importantly, in addition to stabilizing the olefin complex **C**, electron donation from NHC's is expected to accelerate the oxidative addition required for metallacyclobutane formation.

The dramatic decrease in initiation upon substitution of phosphine ligands with N-heterocyclic carbenes is much more difficult to rationalize. X-ray crystallographic studies of these complexes suggest that this is not a ground-state effect. A comparison of crystal structures reveals that the Ru−PCy_3 distance barely changes upon substituting the trans ligand from PCy_3 to IMes (the Ru−PCy_3 distances in **1** are 2.4097(6) and 2.4221(6) Å[45] and the Ru−PCy_3 distance in **14** = 2.419(3) Å).[9] The 640-fold difference in k_1 between these two catalysts may reflect different reorganizational energies associated with the transition states for phosphine dissociation. Alternatively, the variation in initiation rates may simply be the result of a steric effect. Although both PCy_3 and IMes (and $IMesH_2$) are large ligands, the distribution of steric bulk about the ruthenium center is dramatically different in each case.[11] These differential steric distributions may lead to a destabilizing interaction in complexes **1**−**7** or a stabilizing interaction in **8**−**14** which changes the activation energy required for phosphine loss. We anticipate that future studies of k_1 as a function of NHC ligand (where the steric and electronic parameters of this ligand are varied substantially) will provide further insights into the origin of this important effect.

Table 6. Values of k_{rel} for ROMP of COD by Selected Catalysts[a]

catalyst	[Ru] (mM)	COD:Ru	k_{rel}
8	5	300	1.0
9	5	300	1.4
10	5	300	1.4
11	0.05	30 000	0.5
13	5	300	6×10^{-4}

[a] Reaction kinetics measured by ^1H NMR spectroscopy in CD_2Cl_2 at 20 °C.

(2) Phosphine Ligand (PR_3). Changing the phosphine ligand (PR_3) in the $IMesH_2$-coordinated catalysts has a dramatic effect on both catalyst initiation and on catalyst activity. For example, replacing the PCy_3 of catalyst **8** with PPh_3 (**11**) leads to an increase in k_1 of over 2 orders of magnitude. This effect may be related to the lower basicity of the PPh_3 ligand relative to PCy_3 (the pK_a's of the conjugate acids are 2.73 and 9.7, respectively),[46] since a less electron donating phosphine is generally expected to be more labile. Interestingly, however, the PBn_3 complex **12** initiates at almost the same rate as complex **8**, despite the fact that PBn_3 (pK_a = 6.0) is significantly less basic than PCy_3.[46] This result clearly indicates there is not a linear correlation between phosphine pK_a and k_1, and the complexities of the steric and electronic changes resulting from phosphine variation in these systems are still under investigation. Importantly, the PPh_3 catalyst **11** polymerizes COD more than 50 times faster than the PCy_3 complex **8**.[39] A comparison of the k_{-1}/k_2 ratios for these two catalysts (k_{-1}/k_2 = 1.25 and 2.2 for **8** and **11**, respectively) indicates that this result is almost completely due to the improved initiation efficiency of **11**.

(3) Halide Ligand (X). The halide ligands also have a significant impact on the initiation rates of the catalysts $L(PR_3)(X)_2Ru{=}CHR$[1]. In both the bis-phosphine complexes (**1** and **3**) and the $IMesH_2$ complexes (**8** and **10**), changing the X-type ligands from chloride to iodide leads to an approximately 250-fold increase in initiation. (Changing from chloride to bromide results in a much smaller, 3-fold increase in k_1.) We believe that the increase in initiation is predominantly due to the increase in steric bulk upon moving from chloride to iodide. [The ionic radii of Cl^- and I^- are 167 pm and 206 pm, and the covalent radii of Cl and I are 99 pm and 133 pm, respectively.[47]] The larger size of the latter is expected to increase steric crowding at the ruthenium center, thus promoting PR_3 dissociation. Electronics may also play a role in these systems; however, cis electronic effects on dissociative ligand substitution reactions are generally relatively small.[47] Notably, alkoxide X-type ligands are even larger and more electron donating than iodide ligands; in fact, alkoxides are often formally counted as XL ligands, donating *three* electrons to a metal center.[48] We have shown previously that replacing the chlorides of **1** with *tert*-butoxides results in the generation of $(PCy_3)(O^tBu)_2Ru{=}CHPh$ (which can be considered an analogue of **B**) and free PCy_3.[26] The stability of this 4-coordinate *tert*-butoxide adduct clearly demonstrates that the appropriate choice of X-type ligand can effectively promote complete phosphine dissociation.

While the di-iodo catalysts **3** and **10** initiate efficiently, their olefin metathesis activities are comparable to, or even lower

(41) Investigations on this topic are currently in progress. Benitez, D.; Grubbs, R. H. Unpublished results.

(42) The pK_a of 1,3-diisopropyl-4,5-dimethylimidazol-2-ylidene (an NHC closely related to the IMes ligand) is 26. Alder, R. W.; Allen, P. R.; Williams, S. J. *J. Chem. Soc., Chem. Commun.* **1995**, 1267.

(43) Lappert, M. F. *J. Organomet. Chem.* **1975**, *100*, 139.

(44) McGuinness, D. S.; Cavell, K. J.; Skeleton, B. W.; White, A. H. *Organometallics* **1999**, *18*, 1596.

(45) Trnka, T. M.; Henling, L. M.; Grubbs, R. H. Unpublished results.

(46) Streuli, C. A. *Anal. Chem.* **1960**, *32*, 985.

(47) Huheey, J. E.; Keiter, E. A.; Keiter, R. L. *Inorganic Chemistry: Principles of Structure and Reactivity*; Harper Collins: New York, 1993; Chapter 13.

(48) Crabtree, R. H. *The Organometallic Chemistry of the Transition Metals*; John Wiley and Sons: New York, 1994.

than,[4a] those of the parent di-chloride complexes. The moderate olefin metathesis activities of **3** and **10** are related to the k_{-1} to k_2 ratios in these systems. In both the bis-phosphine and the $IMesH_2$ catalyst series, moving from the di-chloride to the di-iodide complex leads to an approximately 100-fold increase in k_{-1}/k_2. The reasons behind this large shift in k_{-1}/k_2 are poorly understood at this time, since it is impossible to separate the effects of the two rate constants. One possible explanation involves the suggestion that olefin coordination requires a trans to cis isomerization of the X-type ligands.[4a] This is might be less favorable when the X-ligands are sterically large and could lead to a decrease in k_2 for the di-iodo catalysts.

(4) Carbene Ligand (R^1). The R^1 ligand also has a large influence on the initiation rates of these catalysts, and k_1 increases substantially as R^1 is changed from H (**4**) to $CHCHC(Me)_2$ (**6**) to Ph (**1**) to CH_2CH_3 (**5**). Earlier studies of initiation in ruthenium olefin metathesis catalysts (using different methodology) showed similar trends in the initiation rate as a function of R^1.[2,4b] These results can be rationalized on the basis of the steric and electronic features of the R^1 substituent. Sterically bulky and electron-donating R^1 groups (e.g., alkyl) lead to higher initiation rates because they more effectively promote phosphine dissociation. In contrast, small and electronically neutral groups (e.g., H) are less effective at labilizing the phosphine ligand.[4b] The effect of R^1 is significant because, unlike the other ligands, this substituent can change throughout an olefin metathesis reaction. An alkylidene moiety is generated after one turnover of a typical ring opening metathesis polymerization and becomes the propagating species. Similarly, a ruthenium methylidene is generated upon initiation of ring closing and cross-metathesis reactions as well as during the acyclic diene metathesis (ADMET) polymerization of terminal olefins.

It is particularly important to point out that the methylidene complexes **4** and especially **13** are *extremely poor initiators* for olefin metathesis reactions at ambient temperatures. Catalyst **13** is an active olefin metathesis catalyst in its phosphine-free form, and multiple catalytic turnovers can be achieved when it is generated in situ from **8**. However, when $(IMesH_2)(Cl)_2Ru{=}CH_2$ is trapped with free PCy_3, it is essentially incapable of re-entering the olefin metathesis catalytic cycle. This is manifest in the extremely low activity of **13** in the polymerization of cyclooctadiene. Because of the slow initiation rates of **4** and **13**, the formation of these complexes should be avoided if at all possible. In many instances, substrate design can be utilized to limit the generation of methylidene intermediates.[49] Substitution of the X and/or PR_3 ligands of **4** or **13** should provide an additional means of improving the initiation efficiencies of these catalysts.

Implications for Olefin Metathesis Reactions. The results described herein have significant implications for the selection and implementation of current olefin metathesis catalysts, as well as for the design of new catalysts and substrates for olefin metathesis reactions.

(1) Catalyst Loadings. A first consideration involves the catalyst loading required for a metathesis polymerization and/or an organic reaction. Lower catalyst loadings facilitate the development of more cost efficient and atom economical processes[50] and make metathesis catalysts more attractive for processes in which residual metal contamination is undesirable. When catalyst initiation is inefficient (as for complex **8** and particularly **13**), the majority of catalyst added to a given reaction remains unused.[51] Faster initiation rates permit a decrease in catalyst loading while maintaining high catalytic olefin metathesis activity. For this reason, the new complexes **10** and **11** are excellent alternatives to **8** for wide variety of catalytic applications. These complexes maintain the superior activity and functional group tolerance of the parent catalyst **8** (in fact, the active species, $(IMesH_2)(Cl)_2Ru{=}CHPh$, for **11** is identical to that in **8**) but initiate almost 2 orders of magnitude faster. As shown in Table 6, the catalyst loading of **11** can be lowered at least 50-fold relative to that of **8** to achieve similar levels of activity for the ROMP of cyclooctadiene.[39]

(2) Kinetic Selectivity. Faster initiation rates also allow for catalysis at lower temperatures than were previously viable. Lowering the temperature is particularly advantageous for the development of selective olefin metathesis reactions. There is intense current interest in the selective formation of either cis or trans olefinic products, as well as in the development of chiral catalysts for the kinetic resolution of racemic olefins.[52,53] However, secondary metathesis events are known to occur readily in these systems and may erode the kinetic selectivity of the catalysts.[54] The development of catalysts that initiate and propagate olefin metathesis at lower temperatures should provide a versatile tool for the optimization of selectivity in metathesis reactions.

(3) Catalyst Decomposition Rates. We believe that the initiation kinetics of catalysts **1**−**14** may also be related to the decomposition rates of these complexes. The thermal decomposition of complexes **1** and **5** has been studied in detail and has been proposed to occur via phosphine dissociation followed by bimolecular coupling of two 4-coordinate ruthenium fragments.[55] These results suggest that catalyst initiation and decomposition in these systems proceed through a common intermediate, **B**. In general, it has been observed that NHC-coordinated complexes exhibit dramatically improved thermal stabilities relative to their bis-phosphine analogues. For example, Nolan and co-workers have demonstrated that complex **14** shows no signs of decomposition after 1 h at 100 °C in toluene-d_8.[56] (Under the same conditions, complex **1** is 75% decomposed.) This remarkable stability was originally attributed to steric and electronic stabilization of the 14-electron intermediate, $IMes(Cl)_2Ru{=}CHPh$, by the IMes ligand.[56] While such stabilization may take place, we suggest that the thermal longevity of **14** (and related NHC complexes) is predominantly due to reduced rates of phosphine dissociation in **14** relative to **1**. Since decomposition is second order in **B**, the rate of decomposition is extremely sensitive to the concentration of **B** in solution, particularly in the absence of olefinic substrates.[55]

Notably, the methylidene complexes **4** and **13** decompose relatively rapidly despite exhibiting very slow rates of initiation. However, both of these complexes appear to decompose by a different pathway than ruthenium alkylidenes and benzylidenes. The decomposition of **4** and **13** is *not* inhibited by the addition

(49) Kirkland, T. A.; Lynn, D. M.; Grubbs, R. H. *J. Org. Chem.* **1998**, *63*, 9904.

(50) Trost, B. M. *Science* **1991**, *254*, 1471.

(51) The low initiation efficiency of **8**, **13**, and **14** suggests that attempts to recycle these catalysts using "boomerang" polymer supports will only result in the recovery of un-initiated **8**. (a) Ahmed, M.; Arnauld, T.; Barrett, A. G. M.; Braddock, D. C.; Procopiou, P. A. *Synlett* **2000**, *7*, 1007. (b) Jafarpour, L.; Nolan, S. P. *Org. Lett.* **2000**, *2*, 4075.

(52) Fujimura, O.; Grubbs, R. H. *J. Am. Chem. Soc.* **1996**, *118*, 2499.

(53) Alexander, J. B.; La, D. S.; Cefalo, D. R.; Hoveyda, A. H.; Schrock, R. R. *J. Am. Chem. Soc.* **1998**, *120*, 4041.

(54) Lee, C. W.; Grubbs, R. H. *Org. Lett.* **2000**, *2*, 2145.

(55) Ulman, M.; Grubbs, R. H. *J. Org. Chem.* **1999**, *64*, 7202.

(56) Huang, J.; Schanz, H. J.; Stevens, E. D.; Nolan, S. P. *Organometallics* **1999**, *18*, 5375.

of free PCy_3.[57] Furthermore, the decomposition of **4** has been shown to exhibit *first-order* kinetics.[55] On the basis of these results, methylidene decomposition has been proposed to occur via intramolecular C−H activation of an L-type ligand, rather than involving the intermediate **B**. In any case, a quantitative investigation of the correlation between k_B and decomposition rate in all of the catalysts **1**−**14** is currently underway.

(4) Polymerization Reactions. A final important implication of these mechanistic studies involves the control of molecular weight distributions in ring opening metathesis polymerizations. It has been observed that the polymerization of highly strained monomers with catalyst **1**, and particularly **8**, results in products with broad molecular weight distributions.[2,15,58] These distributions are the result of a large disparity between the rate of initiation (k_1) and the rate of propagation (k_P) of a polymerization reaction. (Using both catalysts **1** and **8**, $k_1 \ll k_P$ for many monomers.) New procedures for decreasing k_P and/or for increasing k_1 should result in dramatically narrowed polydispersities (PDI's). The mechanism outlined in Scheme 5 suggests a facile method for achieving the former. The addition of free PR_3 to a polymerization will not affect k_1, since k_1 is independent of [PR_3]. However, free phosphine will decrease the rate of propagation by lowering the number of catalytic turnovers that occur before the active species is trapped with free PR_3 (effectively increasing k_{-1}[PR_3] relative to k_2[olefin]). Alternatively, our studies suggest methods for increasing k_1 by modifying either the X-type ligands or the phosphine ligands of catalysts **1** and **8**. Implementation of both of these strategies has proven successful for lowering PDIs in ruthenium-catalyzed ROMP reactions.[59]

In summary, the reactivity of a series of ruthenium metathesis catalysts has been studied in detail. The multistep nature of the olefin metathesis reaction renders mapping the entire reaction coordinate an extremely challenging endeavor. However, this investigation has brought us a few steps closer to understanding the subtle effects of ligand variation on ligand substitution kinetics as well as on catalyst initiation and activity in these ruthenium-based systems. Our studies also provide some insights into methods for tuning both reaction conditions and ligands in order to achieve specific catalytic properties. Many of the subtle and surprising factors governing ligand effects (particularly those involving N-heterocyclic carbenes) in these systems have yet to be unraveled.

Experimental Section

General Procedures. Manipulation of organometallic compounds was performed using standard Schlenk techniques under an atmosphere of dry argon or in a nitrogen-filled Vacuum Atmospheres drybox (O_2 < 2 ppm). NMR spectra were recorded on a Varian Inova (499.85 MHz for ^{1}H; 202.34 MHz for ^{31}P; 125.69 MHz for ^{13}C) or on a Varian Mercury 300 (299.817 for ^{1}H; 121.39 MHz for ^{31}P; 74.45 MHz for ^{13}C). ^{31}P NMR spectra were referenced using H_3PO_4 (δ = 0 ppm) as an external standard. UV−vis spectra were recorded on an HP 8452A diode array spectrophotometer. Elemental analyses were performed at Midwest Microlabs (Indianapolis, IN).

Materials and Methods. Pentane, methylene chloride, diethyl ether, toluene, benzene, and benzene-d_6 were dried by passage through solvent purification columns.[60] Toluene-d_8 and THF-d_8 were dried by vacuum transfer from Na/benzophenone. CD_2Cl_2, pyridine, and ethyl vinyl ether were dried by vacuum transfer from CaH_2. All phosphines were obtained from commercial sources and used as received. Silica gel was obtained from TSI. Ruthenium complexes **1**,[2] **2**,[4a] **3**,[4a] **4**,[2] **5**,[2] **6**,[61] **7**,[62] **8**,[6] and **14**[63] as well as the [$IMesH_2$]BF_4 salt[8b] were prepared according to literature procedures.

($IMesH_2$)(PCy_3)$(Br)_2$Ru=CHPh (9). [$IMesH_2$]BF_4 (115 mg, 0.29 mmol) and KO^{t}Bu (30 mg, 0.27 mmol) were combined in benzene (2 mL), and the resulting yellow suspension was stirred for 1 h. To this suspension was added a solution of complex **2** (220 mg, 0.24 mmol) in benzene (8 mL). The reaction was heated to 50 °C for 18 h and then cooled to room temperature. The resulting suspension was filtered through a plug of Celite, and the benzene was reduced to 2 mL under vacuum. The product was purified by column chromatography (4:1 pentane/diethyl ether) according to the procedure of Hoveyda[64] to afford **9** as a light pink powder (147 mg, 65% yield). ^{31}P{^{1}H} NMR (C_6D_6): δ 30.83 (s). ^{1}H NMR (C_6D_6): δ 19.87 (s, 1H, Ru=C*H*Ph), 9.75 (br s, 1H, ortho C*H*), 7.5−7.0 (br multiple peaks, 6H, meta C*H*, para C*H*, ortho C*H*, and Mes C*H*), 6.70 (br s, 1H, Mes C*H*), 6.10 (br s, 1H, Mes C*H*), 3.55 (br m, 4H, CH_2CH_2), 2.44 (s, 3H, para CH_3), 2.06 (s, 3H, para CH_3), 3.01−1.33 (br multiple peaks, 45 H, PCy_3 and ortho CH_3). ^{13}C{^{1}H} NMR (C_6D_6): δ 296.92 (m, Ru=*C*HPh), 222.31 (d, Ru-*C*(N)$_2$, J_{CP} = 78 Hz), 152.37, 139.40, 138.57, 138.07, 137.92, 137.59, 136.34, 130.61, 129.81, 127.94, 52.72 (d, J_{CP} = 3 Hz), 51.70 (d, J_{CP} = 2 Hz), 33.07, 30.38, 28.59, 28.51, 26.95, 21.91, 21.48, 21.32, 19.91. Anal. Calcd for $C_{46}H_{65}N_2Br_2PRu$: C, 58.91; H, 6.99; N, 2.99. Found: C, 59.25; H, 7.09; N, 2.97.

($IMesH_2$)(PCy_3)$(I)_2$Ru=CHPh (10). Complex **8** (350 mg, 0.41 mmol) and NaI (1.23 g, 8.2 mmol) were combined in THF (15 mL), and the reaction mixture was stirred for 8 h. The solvent was removed under vacuum, and the green residue was taken up in benzene (10 mL). The resulting suspension was filtered through a plug of Celite, and the olive green solution was concentrated under vacuum to yield complex **10** as a green powder (320 mg, 75% yield). ^{31}P{^{1}H} NMR (CD_2Cl_2): δ 30.84 (s). ^{1}H NMR (CD_2Cl_2): δ 19.09 (s, 1H, Ru=C*H*Ph), 7.90−6.94 (br multiple peaks, 8H, ortho C*H*, meta C*H*, para C*H*, and Mes C*H*), 6.25 (br s, 1H, Mes C*H*), 3.98 (br m, 4H, CH_2CH_2), 2.71−2.34 (multiple peaks, 15 H, PCy_3 and Mes CH_3), 2.28 (s, 3H, Mes CH_3), 1.85 (s, 3H, Mes CH_3), 1.56−0.90 (m, 30H, PCy_3).[65] ^{13}C{^{1}H} NMR (C_7D_8): δ 302.34 (m, Ru=*C*HPh), 223.01 (d, Ru-*C*(N)$_2$, J_{CP} = 76 Hz), 152.24, 138.44, 138.04, 137.13, 136.36, 130.27, 129.57, 128.45, 127.33, 126.85, 52.67 (d, J_{CP} = 3 Hz), 51.78 (d, J_{CP} = 1 Hz), 34.84, 34.70, 30.80, 27.28, 27.28, 26.69, 23.54, 20.99, 20.87. Anal. Calcd for $C_{46}H_{65}N_2I_2PRu$: C, 53.54; H, 6.35; N, 2.71. Found: C, 53.68; H, 6.32; N, 2.40.

($IMesH_2$)($C_5H_5N)_2(Cl)_2$Ru=CHPh.[66,67] Complex **8** (1.1 g, 1.3 mmol) was dissolved in toluene, and pyridine (10 mL) was added. The reaction was stirred for 10 min during which time a color change from pink to bright green was observed. The reaction mixture was cannula transferred into 75 mL of cold (0 °C) pentane, and a green sold precipitated. The precipitate was filtered, washed with 4 × 20 mL of pentane, and dried under vacuum to afford ($IMesH_2$)($C_5H_5N)_2(Cl)_2$-Ru=CHPh as a green powder (0.75 g, 80% yield). Samples for elemental analysis were prepared by recrystallization from C_6H_6/pentane followed by drying under vacuum. These samples analyze as the mono-

(57) Ulman, M. Ph.D. Thesis, California Institute of Technology, 2000.
(58) Robson, D. A.; Gibson, V. C.; Davies, R. G.; North, M. *Macromolecules* **1999**, *32*, 6371.
(59) Bielawski, C. W.; Grubbs, R. H., manuscript in preparation.
(60) Pangborn, A. B.; Giardello, M. A.; Grubbs, R. H.; Rosen, R. K.; Timmers, F. J. *Organometallics* **1996**, *15*, 1518.
(61) Wilhelm, T. E.; Belderrain, T. R.; Brown, S. N.; Grubbs, R. H. *Organometallics* **1997**, *16*, 3867.
(62) Complex **7** was prepared by methodology analogous to that used to prepare **6**. Wilhelm, T. E. Ph.D. Thesis, California Institute of Technology, 1998.
(63) Jafarpour, L.; Nolan, S. P. *Organometallics* **2000**, *19*, 2055.
(64) Garber, S. B.; Kingsbury, J. S.; Gray, B. L.; Hoveyda, A. H. *J. Am. Chem. Soc.* **2000**, *122*, 8168.
(65) Minor alkylidene peaks are also observed by ^{1}H NMR spectroscopy at 18.14 and 17.17 ppm (~5% of total) in analytically pure samples of **10**. These peaks disappear upon the addition of free PCy_3, suggesting that they *may* correspond to phosphine-dissociated catalyst species. Further investigation of this phenomenon is underway.
(66) ($IMesH_2$)($C_5H_5N)_2(Cl)_2$Ru=CHPh was prepared by methodology analogous to that used to prepare the phosphine analogue−(PCy_3)-($C_5H_5N)_2(Cl)_2$Ru=CHPh. Dias, E. L. Ph.D. Thesis, California Institute of Technology, 1998.
(67) Further details concerning the synthesis and reactivity of $IMesH_2$-($C_5H_5N)_2(Cl)_2$Ru=CHPh will be reported elsewhere. Sanford, M. S.; Love, J. A.; Henling, L. M.; Day, M. W.; Grubbs, R. H., manuscript in preparation.

pyridine adduct ($IMesH_2$)(C_5H_5N)($Cl)_2$Ru=CHPh, probably due to loss of pyridine under vacuum. ^{1}H NMR (C_6D_6): δ 19.67 (s, 1H, C*H*Ph), 8.84 (br. s, 2H, pyridine), 8.39 (br. s, 2H, pyridine), 8.07 (d, 2H, ortho C*H*, J_{HH} = 8 Hz), 7.15 (t, 1H, para C*H*, J_{HH} = 7 Hz), 6.83−6.04 (br mulitiple peaks, 9H, pyridine, and Mes C*H*), 3.37 (br d, 4H, CH_2CH_2), 2.79 (br s, 6H, Mes CH_3), 2.45 (br s, 6H, Mes CH_3), 2.04 (br s, 6H, Mes CH_3). ^{13}C{^{1}H} NMR (C_6D_6): δ 314.90 (m, Ru=*C*HPh), 219.10 (s, Ru-*C*$(N)_2$), 152.94, 150.84, 139.92, 138.38, 136.87, 135.99, 134.97, 131.10, 130.11, 129.88, 128.69, 123.38, 51.98, 51.37, 21.39, 20.96, 19.32. Anal. Calcd for $C_{33}H_{37}N_3Cl_2Ru$: C, 61.20; H, 5.76; N, 6.49. Found: C, 61.25; H, 5.76; N, 6.58.

($IMesH_2$)(PPh_3)($Cl)_2$Ru=CHPh (11). ($IMesH_2$)($C_5H_5N)_2$($Cl)_2$Ru=CHPh (150 mg, 0.21 mmol) and PPh_3 (76 mg, 0.28 mmol) were combined in benzene (10 mL), and the reaction mixture was stirred for 10 min. The solvent was removed under vacuum, and the resulting brown residue was washed with 4 × 20 mL pentane and dried in vacuo. Complex **11** was obtained as a brownish powder (125 mg, 73% yield). ^{31}P{^{1}H} NMR (C_6D_6): δ 37.7 (s). ^{1}H NMR (C_7D_8): δ 19.60 (s, 1H, Ru=C*H*Ph), 7.70 (d, 2H, ortho C*H*, J_{HH} = 8 Hz), 7.29−6.71 (multiple peaks, 20H, P*Ph*$_3$, para C*H*, meta C*H*, and Mes C*H*), 6.27 (s, 2H, Mes C*H*), 3.39 (m, 4H, CH_2CH_2), 2.74 (s, 6H, ortho CH_3), 2.34 (s, 6H, ortho CH_3), 2.23 (s, 3H, para CH_3), 1.91 (s, 3H, para CH_3). ^{13}C{^{1}H} NMR (C_6D_6): δ 305.34 (m, Ru=*C*HPh), 219.57 (d, Ru-*C*$(N)_2$, J_{CP} = 92 Hz), 151.69 (d, J_{CP} = 4 Hz), 139.68, 138.35, 138.10, 138.97, 137.78, 135.89, 135.21, 135.13, 131.96, 131.65, 131.36, 130.47, 129.83, 129.59 (d, J_{CP} = 2 Hz), 129.15, 128.92, 128.68, 128.00, 52.11 (d, J_{CP} = 4 Hz), 51.44 (d, J_{CP} = 2 Hz), 21.67, 21.35, 21.04, 19.21. Anal. Calcd for $C_{46}H_{47}N_2Cl_2PRu$: C, 66.50; H, 5.70; N, 3.37. Found: C, 67.18; H, 5.81; N, 3.31.

($IMesH_2$)(PBn_3)($Cl)_2$Ru=CHPh (12). ($IMesH_2$)($C_5H_5N)_2$($Cl)_2$Ru=CHPh (150 mg, 0.21 mmol) and PBn_3 (88 mg, 0.29 mmol) were combined in benzene (10 mL), and the reaction mixture was stirred for 10 min. The solvent was removed under vacuum, and the resulting brown residue was washed with 4 × 20 mL pentane and dried *in vacuo*. Complex **12** was obtained as a brown-pink powder (130 mg, 73% yield). ^{31}P{^{1}H} NMR (C_6D_6): δ 34.7 (s). ^{1}H NMR (C_6D_6): δ 19.31 (s, 1H, Ru=C*H*Ph), 8.31 (d, 2H, ortho C*H*, J_{HH} = 7 Hz,), 7.36 (7, 1H, para C*H*, J_{HH} = 7.0 Hz), 7.16 (br s, 19H, P(CH_2*Ph*$)_3$, meta C*H*, Mes C*H*), 6.64 (s, 2H, Mes C*H*), 3.77 (m, 2H, CH_2CH_2), 3.64 (m, 2H, CH_2CH_2), 3.29 (d, 6H, benzyl CH_2, J_{HP} = 7 Hz), 3.18 (s, 6H, ortho CH_3), 2.78 (s, 6H, ortho CH_3), 2.18 (s, 3H, para CH_3), 2.12 (s, 3H, para CH_3). ^{13}C{^{1}H} NMR (C_6D_6): δ 297.50 (m, Ru=*C*HPh), 222.30 (d, Ru-*C*$(N)_2$, J_{CP} = 85 Hz), 151.52, 140.31, 139.54, 137.94, 137.77, 137.30, 135.45, 135.42, 135.39, 131.27, 131.24, 131.21, 130.21, 129.72, 129.00, 126.42, 126.40, 51.72 (d, J_{CP} = 1 Hz), 51.52 (d, J_{CP} = 4 Hz), 25.80, 25.68, 21.36, 21.20, 21.11, 19.13. Anal. Calcd for $C_{49}H_{53}N_2Cl_2PRu$: C, 67.42; H, 6.12; N, 3.21. Found: C, 67.70; H, 6.20; N, 3.26.

($IMesH_2$)(PCy_3))($Cl)_2$Ru=CH_2 (13). Complex **8** (300 mg, 0.35 mmol) was dissolved in benzene (10 mL) and pressurized with ∼1.5 atm of ethylene. The reaction mixture was stirred at 50 °C for 90 min during which time a color change from pink to dark brown was observed. The brown solution was cooled to room temperature, and the product was purified by column chromatography (gradient elution: 100% pentane to 8:1 pentane/diethyl ether) according to the procedure of Hoveyda[64] to afford an orange-yellow solid (97 mg, 36% yield). ^{31}P{^{1}H} NMR (C_6D_6): δ 38.6 (s). ^{1}H NMR (C_6D_6): δ 18.41 (s, 2H, Ru=CH_2), 6.92 (s, 2H, Mes C*H*), 6.70 (s, 2H, Mes C*H*), 3.22 (m, 4H, CH_2CH_2), 2.78 (s, 6H, ortho CH_3), 2.53 (s, 6H, ortho CH_3), 2.37 (m, 3H, P*Cy*$_3$), 2.18 (s, 3H, para CH_3), 2.10 (s, 3H, para CH_3), 1.61 (m, 12H, P*Cy*$_3$), 1.10 (m, 18H, P*Cy*$_3$). ^{13}C{^{1}H} NMR (C_6D_6): δ 294.75 (d, Ru=*C*H_2, J_{CP} = 10 Hz), 222.52 (d, Ru-*C*$(N)_2$, J_{CP} = 75 Hz), 139.59, 138.95, 138.41, 138.11, 137.76, 135.33, 130.49, 130.00, 128.91, 128.67, 128.03, 127.84, 51.97 (d, J_{CP} = 3 Hz), 50.33 (d, J_{CP} = 1 Hz), 31.03, 30.89, 29.51, 28.37, 28.29, 28.29, 27.03, 21.53 (d, J_{CP} = 3 Hz), 20.42, 19.42. Anal. Calcd for $C_{40}H_{61}N_2Cl_2PRu$: C, 62.16; H, 7.96; N, 3.62. Found: C, 61.12; H, 7.75; N, 3.64.

Magnetization Transfer Experiments. The ruthenium alkylidene (0.024 mmol) and PCy_3 (in equivalents relative to [Ru]) were combined in toluene-d_8 (600 μL) in an NMR tube, and the resulting solution was allowed to thermally equilibrate in the NMR probe. The free phosphine resonance was selectively inverted using the DANTE pulse sequence, and after variable mixing times (between 0.00003 and 50 s), a nonselective 90° pulse was applied and an FID recorded. ^{1}H decoupling was applied during the 90° pulse. Spectra were collected as 4−8 transients with relaxation delays between 30 and 50 s. The peak heights of the free and bound phosphine at variable mixing times were analyzed using the computer program CIFIT in order to obtain the exchange rate of bound phosphine with free phosphine (k_B). Values for the T_1's for the free and bound phosphine were also obtained in this analysis, and the results are summarized in Table S1. The relaxation times (T_1) for complexes **1**−**14** as well as for free PCy_3 were determined independently using standard inversion recovery experiments, and the results are summarized in Table S2. Eyring plots for catalysts **1**−**14** are shown in Figures S1−S11.

NMR Initiation Kinetics. The ruthenium alkylidene (0.0106 mmol) was dissolved in toluene-d_8 (600 μL) in an NMR tube fitted with a screw cap containing a rubber septum. The resulting solution was allowed to equilibrate in the NMR probe at the appropriate temperature, and ethyl vinyl ether (in equivalents relative to [Ru]) was injected into the NMR tube neat. Reactions were monitored by measuring the peak heights of the starting alkylidene as a function of time over at least 3 half-lives. The data were fitted to a first-order exponential using Varian kinetics software.[68]

UV−Vis Initiation Kinetics. In a cuvette fitted with a rubber septum, a solution of ethyl vinyl ether (in equivalents relative to the [Ru]) in toluene (1.6 mL) was prepared. This solution was allowed to thermally equilibrate in the UV−vis spectrometer at the appropriate temperature. To the temperature-equilibrated solution was added 100 μL of a 0.0139 M stock solution of the ruthenium catalyst in toluene. The kinetics of the reaction were followed by monitoring the appearance of the product as a function of time. The data were collected over 5 half-lives, and kinetics traces were fitted to first-order exponentials. Plots of k_{Init} versus [olefin] for catalysts **2**, **5**, and **7** are shown in Figures S12−S14.

$1/k_{obs}$ vs [PCy_3]/[olefin] for Catalysts 1, 2, and 3. Ruthenium catalyst (0.0106 mmol) and PCy_3 (in equivalents relative to [Ru] from a 0.061 M stock solution in toluene-d_8) were combined in an NMR tube fitted with a screw cap containing a rubber septum. The resulting solutions were diluted to a total volume of 600 μL with toluene-d_8. The tubes were allowed to thermally equilibrate in the NMR probe, and the ethyl vinyl ether (in equivalents relative to [Ru]) was injected neat into the NMR tube. Reactions were monitored by measuring the peak heights of the starting alkylidene as a function of time over at least 3 half-lives as described above. Plots of $1/k_{obs}$ as a function of [PCy_3]/[olefin] for complexes **1**, **2**, and **3** are shown in Figures S15−S17.

$1/k_{obs}$ vs [PR_3]/[olefin] for Catalysts 6, 8, 10, 11, and 12. Ruthenium catalyst (0.0106 mmol) and PR_3 (in equivalents relative to [Ru]) were combined in an NMR tube fitted with a screw cap containing a rubber septum. The solids were dissolved in 600 μL of toluene-d_8. Each solution was allowed to thermally equilibrate in the NMR probe, and ethyl vinyl ether (in equivalents relative to [Ru]) was injected neat into the NMR tube. Reactions were monitored by measuring the peak heights of the starting alkylidene as a function of time over at least 3 half-lives as described above. Plots of $1/k_{obs}$ as a function of [PR_3]/[olefin] for complexes **6**, **8**, **10**, **11**, and **12** are shown in Figures S18−S22.

ROMP of Cyclooctadiene. The ruthenium alkylidene (0.003 mmol) was dissolved in CD_2Cl_2 (600 μL) in an NMR tube fitted with a screw cap containing a rubber septum. The resulting solution was allowed to equilibrate in the NMR probe at 20 °C, and COD (0.90 mmol) was injected into the NMR tube neat. Reactions were monitored by measuring the peak heights of the COD olefinic signal as a function of time over at least 3 half-lives. The data were fitted to a first-order exponential using Varian kinetics software.[68] For catalyst **11**, the same procedure was followed with the exception that 0.006 μmol of ruthenium benzylidene was used.

Acknowledgment. The authors would like to thank Dr. Jeff Yoder and Dr. Ola Wendt for assistance with magnetization

(68) *VNMR 6.1B Software*; Varian Associates, Inc.

transfer experiments. Dr. Michael Ulman and Annita Zhong are acknowledged for helpful discussions, and Dr. Steven Goldberg and Dr. Jon Seiders are acknowledged for critical reading of this manuscript. J.A.L. thanks the NIH for a postdoctoral fellowship. This work was supported by the NSF.

Supporting Information Available: Tables of phosphine exchange rate constants, T_1 data, Eyring plots, k_{Init} vs [olefin] plots, and $1/k_{obs}$ vs $[PR_3]$/[olefin] plots. This material is available free of charge via the Internet at http://pubs.acs.org.

JA010624K